Check for updates

Three-dimensional crimped biodegradable poly(lactic acid) fibers prepared *via* melt spinning and controlled structural reorganization

Bo Yang, Rui Wang, [ID] Zhenfeng Dong, Jing Wu, Minxuan Kuang, Gaoling Jin, Huiling Ma, Yang Wang, Qingying Zhang and Xiuqin Zhang [ID] *

Biodegradable three-dimensional crimped fibers were prepared by the side-by-side composite spinning of poly(lactic acid) (PLA) and low-melting point PLA (LM-PLA). The structural variation of the PLA/LM-PLA composite fibers during dry and wet heat treatment was explored systematically. It is shown that crystallization and disorientation were two key factors for the formation of the three-dimensional crimped structure of PLA/LM-PLA side-by-side composite fibers (SSCF). The wet heat-treated fiber has better crimp performance and fluffiness, and the crimp number, crimp ratio and crimp elasticity ratio of the treated PLA/LM-PLA SSCF with good comprehensive properties are 21 per 25 mm, 31.9% and 81.6%, which are similar to those of industrialized PET/PTT three-dimensional crimped fibers. The results of this study shed light on the development of novel three-dimensional crimped fibers with biodegradability.

1 Introduction

Three-dimensional crimped fibers are important in commercial textiles and clothing to imitate the properties of wool, *e.g.* fluffiness, cushion elasticity, and thermal insulation.[1] The self-crimping property of wool results from its unique cross-sectional structure composed of the adhered ortho-cortex and the para-cortex. Synthetic fibers with similar crimped properties have been developed by using two polymers with different thermal-shrinkage, such as poly(ethylene terephthalate) (PET)/poly(trimethylene terephthalate) (PTT), PET/poly(butylene terephthalate) (PBT), PBT/polypropylene (PP), *etc.* Some of the commercial crimped fibers, for example, Invista's T400,[2] which is made from PET and PBT with different shrinkage, are inherently elastic, preserve these properties during normal maintenance and have a softer touch than those of textured polyester fibers. Zhang *et al.*[3] prepared PET side-by-side composite fibers (SSCF) with different spun viscosities. And the fabrics showed excellent drape property. The crimp ratio, and crimp elastic ratio were 12% and 70%, respectively. Yang *et al.*[4] prepared PET/PBT side-by-side fiber "T80", which has the advantages of excellent dyeing performance, stable shrinkage, and high elasticity.

The design of a suitable process is critical for preparing crimped fibers. In particular, a "dumbbell" cross-section structure of the bicomponent fiber is an effective way. Luo

et al.[5] prepared three PTT/PET filaments that have approximately identical monofilament fineness but with different cross-sectional shapes: "dumbbell, gourd, round". It turns out that the dumbbell-shaped cross-section showed the best crimp curvature and elasticity. Since the crimped structure is formed due to the imbalance shrinkage, the parameters of the spinning and draw-setting step decide the morphology of the fibers. Oh *et al.*[6] studied the crimp properties in the melt-spinning and drawing processes of SSCF of PTTs with different viscosities. The shrinkage and birefringence difference increase with the draw ratio, which is closely related to the crystallinity and orientation,[7] thus leading to an increase in the crimp contraction. On the other hand, "wet-treatment" by immersing fibers into water is effective for those water-absorbing fibers. Xiao *et al.*[8] reported that water can promote the mobility of molecular chains of PET/PTT SSCF, resulting in unbalanced disorientation of the fibers and crimped architecture. It was claimed that the crimp properties of PET/PTT SSCF treated in boiled water were better than those treated in the oven at 100 °C. Moreover, the compatibility between the two components is essential for a crimped structure. For example, Zhang *et al.*[9] observed the splitting of the adjacent fibers when choosing the incompatible PET and PA6. However, due to the good compatibility between PET and PTT, composite fibers with crimped structure were obtained.

Poly(lactic acid) (PLA), as one of the biodegradable materials, has comparable strength with polypropylene, can be made into lightweight fabrics which are comfortable,[10] anti-microbial,[11] and suitable for applications in clothing fabrics, *etc.* The advantages included biocompatibility, biodegradability, and biological source of PLA also endow it as an environment-

Beijing Key Laboratory of Clothing Materials R&D and Assessment, Beijing Engineering Research Center of Textile Nanofiber, School of Materials Science & Engineering, Beijing Institute of Fashion Technology, Beijing 100029, China. E-mail: clyzxq@bift. edu.cn; Tel: +86 13520886284

friendly material. However, to the best of our knowledge, there is no report on the three-dimensional crimped PLA fibers so far, although there were many studies on PLA fibers.[12,13] As discussed above, the compatibility[14–17] between the two polymers is essential for composite fibers. Since the best compatible candidate to a polymer is the polymer itself. Meanwhile, using the same polymer to prepare composite fibers has additional advantages such as recycling. Herein, two kinds of PLA that show different melt points were chosen to test the above concept. Side-by-side composite fibers with three-dimensional crimped architecture were successfully prepared. The mechanism of the structure formation is the different crystallization capacity and structural stability of the two PLA materials with different stereoregularity. The prepared fibers have promising potentials in high-end fabrics.

2 Experimental

2.1 Materials

PLA 190 (optical purity = 99.7%, M_w = 11 kg mol^{-1}, T_g = 60.9 °C, T_m = 173.5 °C) and LM-PLA 101 (optical purity = 88.8%, M_w = 8 kg mol^{-1}, T_g = 63.1 °C, T_m = 142.0 °C) was purchased from Zhejiang Haizheng Biomaterial Co. Ltd.

2.2 Preparation of PLA plates

The PLA pellets were dried at 80 °C in a vacuum oven (Binder, Germany) for 12 h. 0.3 mm thick plates of PLA were prepared by hot-pressing with the molding pressure of 4 MPa at 200 °C for 3 min. Subsequently, the samples were cooled down quickly to room temperature, then were cut into dumbbell-shaped with 40 mm in length, 2 mm in width, and 0.3 mm in thickness by using a cutting machine (RR/PCP, Ray-Ran, UK).

The draw-setting process was carried out on a Linkam TST 350 stretching hot stage (Linkam Scientific Instruments, Ltd., UK). The samples were stretched to a strain of 150% with a speed of 50 μm s^{-1} at 75 °C, and annealed at different temperatures. The codes of PLA plates under different stretching conditions are shown in Table 1.

2.3 Preparation of fibers

Equivalent amounts of PLA and LM-PLA were extruded from a spinneret with 24 holes of 0.3 mm diameter at a throughput

rate of 18 ml min^{-1} with a compound spinning machine made by Dalian Synthetic Fiber Research Institute. PLA/LM-PLA side-by-side composite fibers (PLA/LM-PLA SSCF) were collected at a take-up speed of 2000 m min^{-1}. The processing temperatures in each zone of LM-PLA were set at 135 °C (Zone 1), 190 °C (Zone 2), 205 °C (Zone 3), 203 °C (Zone 4), 215 °C (flange) and 220 °C (spinneret) from feed zone to the spinneret. The temperatures in each zone of PLA were set at 160 °C (Zone 1), 205 °C (Zone 2), 200 °C (Zone 3), 210 °C (Zone 4), 215 °C (flange) and 220 °C (spinneret) from feed zone to the spinneret. Then the fibers were further heated and drawn on drafting machine (Tongfeng, China). The draft ratio is 1.5, temperature of roller 1, roller 2 and heat-set were 70 °C, 75 °C and 120 °C, respectively. The fineness of single PLA/LM-PLA SSCF is 0.4 mm and the strength and elongation at break was 3.01 cN per dtex and 15.1%.

2.4 Measurement and characterization

2.4.1 DSC measurements. The thermal properties of PLA and LM-PLA were characterized by DSC with a TA Q2000 (TA Instrument, USA) under the nitrogen atmosphere. The instrument was calibrated with indium before measurements. The weight of each sample was 5–10 mg. The samples were heated–cooled–reheated with a rate of 10 °C min^{-1} within the region of 30–210 °C. The crystallinity degree (X_c) of samples was estimate according to the following equation:

$$X_c = \frac{\Delta H_m - \Delta H_{cc}}{\Delta H_m^0} \times 100\% \tag{1}$$

where ΔH_m and ΔH_{cc} are fusion enthalpy and cold crystallization enthalpy calculated by DSC, ΔH_m^0 was the fusion enthalpy of the completely crystalline PLLA. Here, the value of ΔH_m^0 of PLLA was 93 J g^{-1}.[18]

2.4.2 Morphological analysis. The morphology of the fibers were characterized using a JSM-7500F scanning electron microscope (SEM) (JEOL, Japan). The instrument was operated with an accelerating voltage of 8 kV and a current of 10 μA. The samples were coated with a thin layer of gold.

2.4.3 Sonic velocity orientation analysis. The chain orientation was measured on a SCY-III sonic velocity orientation meter (School of Materials, Donghua University, China). The orientation factor can be estimated by the formula:

Table 1 Codes of PLA plates

Samples	Stretching condition	Annealing temperature (°C)	Code
PLA	Strain: 150%; temperature: 75 °C; speed: 50 μm s^{-1}	60	75-60-1
		70	75-70-1
		80	75-80-1
		90	75-90-1
LM-PLA		60	75-60-2
		70	75-70-2
		80	75-80-2
		90	75-90-2

$$\alpha = 1 - \frac{C_u{}^2}{C^2} \tag{2}$$

where α is orientation factor of fiber, C and C_u is the speed of sound waves in oriented and random orientation fibers, respectively.

2.4.4 X-ray diffraction (XRD) measurements. The crystalline structure and degree of crystallinity were measured by X-ray diffractometer (Bruker AXS D8). The wavelength of the radiation was 0.154 nm. The two-dimensional wide-angle X-ray scattering (2D WAXS) patterns were collected by the two-dimensional detector VANTEG-500. The exposure time was 60 s and the sample-to-detector distance was 85.6 mm. 2D patterns were converted into 1D scattering profiles along the angle 0–360°. The relative fraction of different phases was calculated according to:

$$X_c = \frac{I_c}{I_c + I_{amor}} \tag{3}$$

where I_c and I_{amor} stand for the integral intensities of the peaks of the crystals and amorphous phase, respectively.

The orientation factor of the (110)/(200) crystal plane is calculated according to the Hermans' formula,[19] where Φ is the angle between the normal direction of the crystal plane and the fiber axis.

$$\langle \cos^2 \Phi \rangle = \frac{\int_0^{\frac{\pi}{2}} I(\Phi)\cos^2 \Phi \sin \Phi \mathrm{d}\Phi}{\int_0^{\frac{\pi}{2}} I(\Phi)\sin \Phi \mathrm{d}\Phi} \tag{4}$$

$$f_{(110)/(200)} = \frac{3(\langle \cos^2 \Phi \rangle) - 1}{2} \tag{5}$$

2.4.5 Tensile test. PLA fibers were tested on a QX-2 monofilament strength meter (Shanghai Lipu, Ltd., Shanghai) with clamping distance of 10 mm and drawing speed of 50 mm min⁻¹. 10 parallel measurements were carried out. The average value was recorded.

2.4.6 Crimp property analysis. The crimp feature was performed according to GB/T 14338-2008, the pre-tension of light and heavy is 0.008 cN and 0.3 cN, respectively. A section of heat-treated SSCF was selected for testing randomly.

Measure the length of single filament L_0 under the action of light load of 0.008 cN for 30 s, after the light load and replaced by the heavy load of 0.3 cN, the length was measured and recorded as L_1, then removing the heavy load for 2 min, the length L_2 of the fiber was measured under light load of 0.008 cN.

(1) Crimp ratio (J): it refers to the degree of crimp, which is related to the number and wave depth of crimp structure.

$$J \ (\%) = \frac{L_1 - L_0}{L_1} \times 100\% \tag{6}$$

where L_0 and L_1 were the length (mm) of the fiber measured under light load (0.008 cN) and heavy load (0.3 cN) respectively.

(2) Crimp elastic ratio (J_d): large crimp elastic ratio indicates good crimp stability of elastic yarn, and the formula was as follows:

$$J_d \ (\%) = \frac{L_1 - L_2}{L_1 - L_0} \times 100\% \tag{7}$$

(3) Crimp number (J_n): the crimp number of single fiber within 25 mm, which affects the friction and cohesion between fibers. The calculation formula was as follows:

$$J_n \ (n) = \frac{L_A}{L \times 2} \times 25 \tag{8}$$

where L (mm) was the length of measured fiber; L_A refers to the total number of crimp peaks and valleys in the length L of the single fiber.

3 Results and discussion

3.1 Thermal properties

The DSC curves of PLA and LM-PLA are shown in Fig. 1. During cooling, the absence of crystallization peak indicates poor melt-crystallization ability of both PLA and LM-PLA. However, the second heating curves show clear cold-crystallization and subsequent melting behavior in PLA, suggesting that PLA has better cold-crystallization ability than that of LM-PLA (Fig. 1(b)). The glass transition temperatures (T_g) of PLA and LM-PLA are 60.1 °C and 63.1 °C in the second heating, respectively.

To understand how the samples behave under deformation, the PLA and LM-PLA were further studied by DSC after a stretching treatment. First, the specimens were stretched to
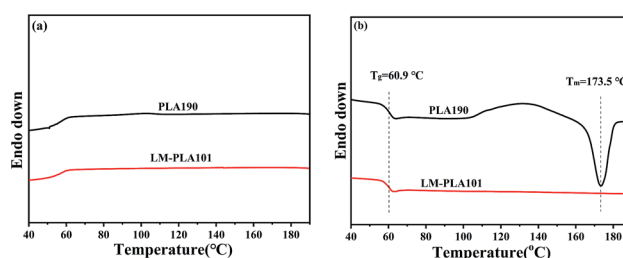

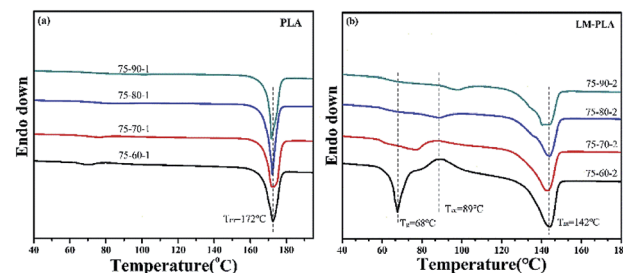Fig. 1 (a) DSC cooling curves and (b) the second heating curves of PLA and LM-PLA samples.

Fig. 2 The first heating curves of PLA and LM-PLA after tensile-heat treatment: (a) PLA samples, (b) LM-PLA samples.
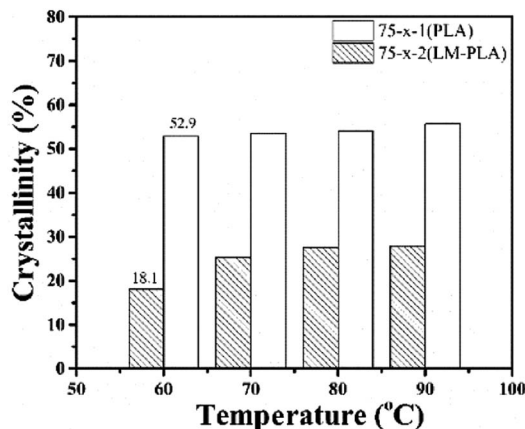
Fig. 3 The crystallinity of PLA and LM-PLA specimens prepared by stretching and subsequently heat treatment at different annealing temperatures.

150% at 75 °C and then annealed at various temperatures as indicated in Fig. 2. PLA shows a melting peak at 172 °C and the crystallinity is about 53%, assuming the melting enthalpy of 93 J g^{-1} for 100% crystalline PLA.[18] No significant difference in crystallinity is observed for different annealing temperatures. On the other hand, the LM-PLA is sensitive to annealing temperature. The 75-60-2 sample exhibits an obvious endothermic peak around the glass transition temperature (T_g) indicating local order structure was formed during the stretching process and the subsequent heat treatment.[20,21] A cold crystallization peak appears at 89 °C. The total crystallinity of PLA and LM-PLA specimens prepared by stretching and subsequently annealing were plotted in Fig. 3. Obviously, PLA shows better crystallization capacity than that of LM-PLA. The different crystallization behavior between PLA and LM-PLA with annealing provides the structural basis for preparing crimped fibers because the shrinkage of the two components would be different.

3.2 Morphologies of PLA/LM-PLA SSCF

PLA/LM-PLA side-by-side composite fibers were prepared under conditions as described in the Experimental section. The fibers show uniform "dumbbell" morphology as shown in Fig. 4(a). The diameter of the fiber is 0.4 mm. Fig. 4(b) shows the side view of the surface of the fiber, where we can see good adhesion between the PLA fiber and LM-PLA fiber. This is a advantage of using the both PLAs to ensure good compatibility.

We are interested in the structure of the fibers. Fig. 5 shows the first heating curve of DSC and 2D WAXS pattern of PLA/LM-
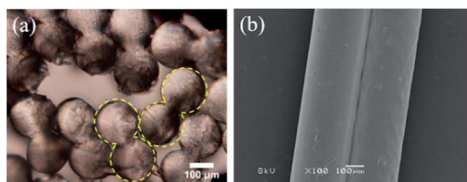

Fig. 4 Photos of PLA/LM-PLA SSCF: (a) fiber cross-section, (b) SEM of the surface of the fiber.
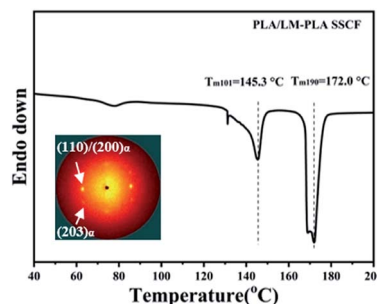

Fig. 5 The first heating curve of DSC and 2D WAXS of PLA/LM-PLA SSCF, the fibers were aligned vertically.

PLA SSCF. Two endothermic peaks at 145.3 °C and 172.0 °C are observed which can be assigned to the melting peaks of LM-PLA and PLA, respectively. No obvious cold crystallization phenomenon was observed. The crystallinity of LM-PLA and PLA components were 26.9% and 55.8%, respectively. The difference in crystallinity between the two components in SSCF, will result in unbalanced shrinkage during subsequent heat treatment, which is the origin of three-dimensional crimped structure.

3.3 Effect of heat treatment

3.3.1 Dry heat treatment. To test the effect of thermal treatment on the unbalanced shrinkage of the compound fibers, the PLA/LM-PLA SSCF were placed in the oven at different temperatures (90 °C, 95 °C, 100 °C, 105 °C, 110 °C) for 30 min without tension. Interestingly, we found that three-dimensional crimped fibers were obtained after the treatment. The morphologies and the crimp properties were shown in Fig. 6 and Table 2 respectively. Among all the tested samples, the specimens annealed at 90 °C and 95 °C show uniform three-dimensional crimped structures, while increased shrinkage and decreased crimp radius were observed at a higher temperature. This may be due to the amorphous softening differences between LM-PLA and PLA.

The crimp properties of dry heat-treated PLA/LM-PLA SSCF are shown in Table 2. At 90 °C, the crimp number, crimp ratio, and crimp elasticity ratio are 20 per 25 mm, 29.9%, and 80.0%, respectively. With increasing dry heat-treatment temperature, no obvious changes in the crimp number of PLA/LM-PLA SSCF can be seen, and the crimp ratio decreased slightly. When the dry heat-treatment temperature increases to 105 °C and 110 °C, the PLA/LM-PLA SSCF stick together because of the viscus flow of the amorphous phase. Therefore, the crimp properties cannot be measured. It is reported that the crimp number, crimp ratio and crimp elasticity ratio of wool were 21 per 25 mm, 7.9% and 90.9%, respectively,[22] and the crimp number, crimp ratio and crimp elasticity ratio of PET/PTT SSCF were 20 per 25 mm, 20%, and 88%.[23] The above results showed that the three-dimensional crimped properties of PLA/LM-PLA SSCF were close to the performance of wool and PET/PTT SSCF.

Fig. 7 reveals the effect of dry heat-treatment on the mechanical properties of PLA/LM-PLA SSCF. The strength of

Table 2 Crimp properties of dry and wet heat-treated PLA/LM-PLA SSCF

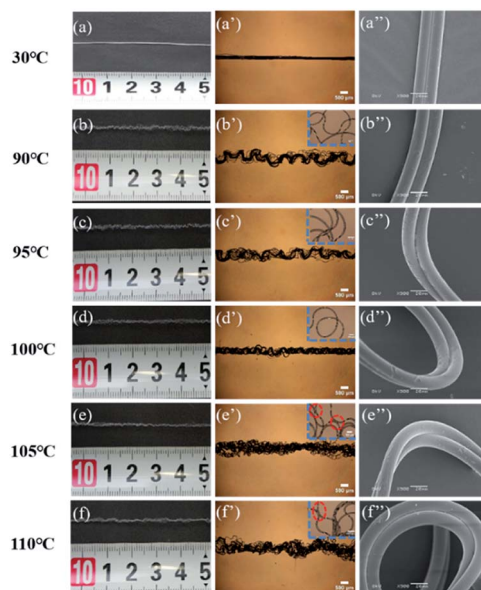| Methods	Temperature (°C)	Crimp number (J_n/25 mm)	Crimp ratio (J/%)	Crimp elastic ratio (J_d/%)
Dry heat treatment	90	20	29.9	80.0
	95	20	29.6	82.6
	100	20	26.2	81.6
Wet heat treatment	60	17	27.5	80.6
	65	21	31.9	81.6
	70	22	25.5	84.2
	75	22	16.1	84.1

Fig. 6 The photos of PLA/LM-PLA SSCF treated by dry heat-treatment at different temperatures, (a–f) digital camera, (a′–f′) optical microscope, and (a″–f″) SEM.

PLA/LM-PLA SSCF is 3.01 cN per dtex. When the dry heated temperature was 90 °C, the strength increased slightly to 3.32 cN per dtex. Further increasing the dry heat-treatment temperature to 100 °C, the strength remained unchanged. According to the above experimental results, the best dry heat-treatment temperature was 90 °C. It is reported that the strength of PET/PTT SSCF was about 2.5 cN per dtex,[24] which is
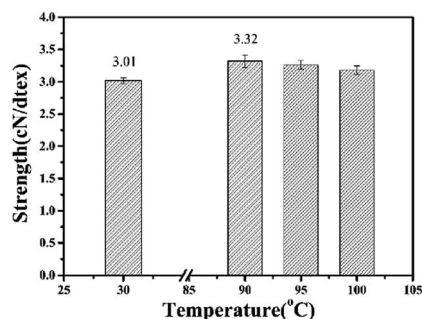

Fig. 7 Effect of dry heat-treatment on the mechanical properties of PLA/LM-PLA SSCF.

lower than that of dry heat-treated PLA/LM-PLA SSCF, showing the better mechanical properties.

3.3.2 Wet heat-treatment. Wet heat-treatment is one of the common methods to obtain the three-dimensional crimped structure. In the treating process, water molecules could enhance the chain mobility, thus the potential shrinkage properties could be fully exerted. The obtained wet heat-treated three-dimensional crimped fibers have better crimp performance[25] and fluffiness.

The PLA/LM-PLA SSCF were treated without tension in a water bath at different temperatures (60 °C, 65 °C, 70 °C, 75 °C, 80 °C) for 30 min, the effect of wet heat-treatment temperature on the three-dimensional crimped structure of the SSCF was investigated, and the results are shown in Fig. 8. When treated at 60 °C and 65 °C, PLA/LM-PLA SSCF obtained a uniform three-dimensional crimped structure, which had good fluffy property comparing with dry heat treatment at 90 °C. According to Table 2, the crimp number, crimp ratio, and crimp elasticity ratio of PLA/LM-PLA SSCF treated at 60 °C were 17 per 25 mm, 27.5% and 80.6%, respectively. When wet heat-treatment temperature increasing to 65 °C, the crimp number, crimp ratio and crimp elasticity ratio of PLA/LM-PLA
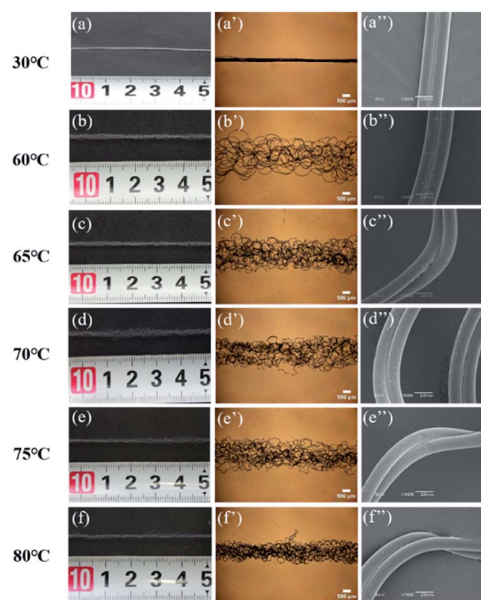

Fig. 8 The photos of PLA/LM-PLA SSCF treated by water different temperatures, (a–f) digital photo, (a′–f′) optical microscope and (a″–f″) SEM.
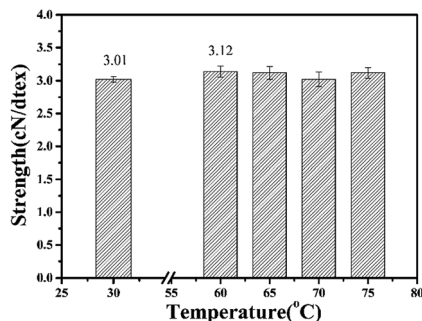
Paper

Fig. 9 Effect of wet heat-treatment on the mechanical properties of PLA/LM-PLA SSCF.
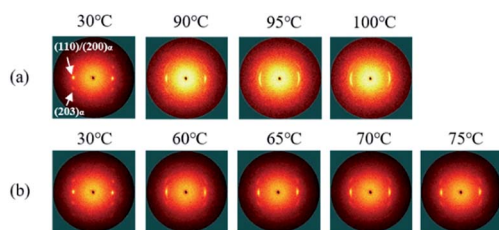

Fig. 10 2D WAXS of heat-treated PLA/LM-PLA SSCF under (a) dry heat treatment and (b) wet heat treatment, the fibers were aligned vertically.

SSCF were 21 per 25 mm, 31.9% and 81.6%, the crimp performance was significantly improved. Further increasing wet heat-treatment temperature to 70–80 °C, PLA/LM-PLA side-by-side composite fiber shrinks sharply, the crimp radius and the fluffiness decreases gradually (Fig. 8(d′–f′)).

Fig. 9 showed the effect of wet heat-treatment temperature on the mechanical properties of PLA/LM-PLA SSCF. It can be seen that the strength of PLA/LM-PLA SSCF treated at 60–75 °C was 3.12 cN per dtex. Compared with the PLA/LM-PLA SSCF with dry heat-treatment at 90 °C, the fibers with wet heat-treatment at 65 °C exhibited better crimping properties and bulkiness. Therefore, the optimal wet-heated temperature for PLA/LM-PLA SSCF was 65 °C.

3.4 Crimped mechanism

The crimped mechanism of SSCF is mainly based on different shrinkage of the two components, which result from structural factors such as crystallization and orientation in semi-crystalline polymers.[26–28] Here, the degree of crystallinity and orientation was measured by WAXS and sonic velocity.

As shown in Fig. 10 and Table 3, when the fibers were dry heat-treated without tension at 90 °C, the length of the diffraction arc increases, and the degree of orientation of (110)/(200) plane decreased from −0.40 to −0.30. The crystallinity of α crystals increased from 27.1% to 30.8%. It indicated that there were some low orientated crystals formed in dry heat-treated fibers. Simultaneously, the orientation factor of the fiber decreased from 0.54 to 0.31 (Fig. 11(a)). In the process of heat-treatment without tension at 90 °C, the chains in the amorphous region of PLA and LM-PLA could move, disorientate, and part of folding chains formed α crystals. The difference of shrinkage property for two components was the key factor for the formation of a uniform three-dimensional crimped structure of the PLA/LM-PLA SSCF,[29,30] which were mediated by the movement ability and crystallization of chains. As shown in Table 3, when heat-treatment temperature further increased from 95 °C to 100 °C, the crystallinity of fibers further increases from 33.4% to 39.6% and the orientation factor of the fiber further decreased from 0.24 to 0.20 (Fig. 11(a)). An increase of shrinkage degree caused by crystallization and disorientation resulted in the formation of three-dimensional crimped structure with low crimp radius (Fig. 6).

As shown in Fig. 10(b) and 11(b), with increasing the wet heat-treatment temperature, the crystallinity in the PLA/LM-PLA SSCF was nearly unchanged, while the orientation factor of PLA/LM-PLA SSCF decreased remarkably. When performed at 60 °C, the degree of orientation decreased from 0.53 to 0.43. With the
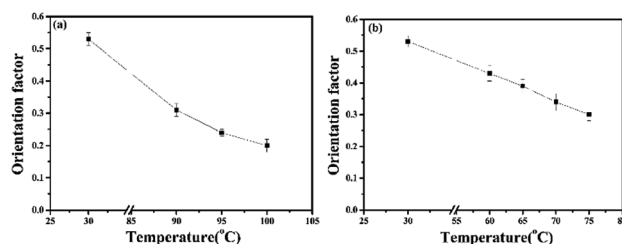

Fig. 11 Relation curves of orientation factor of PLA/LM-PLA SSCF measured by sonic velocity orientation meter: (a) dry heat treatment, (b) wet heat treatment.

Table 3 Crystal information of PLA/LM-PLA SSCF treated under different conditions

Methods	Temperature (°C)	Crystallinity (%)	$f_{(110)/(200)}\alpha$
Untreated	Room temperature (30 °C)	27.1	−0.40
Wet heat treatment	60	27.8	−0.34
	65	27.2	−0.35
	70	28.1	−0.34
	75	28.5	−0.35
Dry heat treatment	90	30.8	−0.30
	95	33.4	−0.22
	100	39.6	−0.24

wet heat-treatment temperature up to 65–75 °C, the orientation factor decreased to 0.3. During the wet heat treatment, hot air and water molecules influenced the motion of the molecular chains in the amorphous region, resulting in more disorientation of wet heat-treated SSCF. Thus, the PLA/LM-PLA SSCF formed three-dimensional crimped structures.

Based on above results, when fibers were heat treated without tension, the PLA and LM-PLA components have different shrinkage ratio. Due to the good compatibility between the PLA and LM-PLA, the PLA fiber and LM-PLA fiber attaches firmly. Therefore, stress is generated at the boundary of PLA and LM-PLA during the heat-treatment. The entire fiber spontaneously bent and twisted to form three-dimensional crimped structure to release the stress. This is expected to be a general reason for the crimped architecture.

4 Conclusions

In this work, biodegradable PLA/LM-PLA SSCF were prepared by melt composite spinning, the effects of dry and wet heat treatment on the structure and properties of PLA/LM-PLA SSCF were investigated systematically. It was observed that the crystallization ability of LM-PLA was much weaker than that of PLA under the same crystallization conditions, which is the key factor that affects the formation of the three-dimensional crimped structure of fibers during heat treatment. The best dry heat treatment temperature is 90 °C, the crimp number, crimp ratio, and crimp elasticity ratio of PLA/LM-PLA is 20 per 25 mm, 29.9%, and 80.0%, respectively. In the wet heat treatment, the motion of LM-PLA chains in the amorphous region caused by hot air and water molecules promoted the formation of the three-dimensional crimped structure. Finally, the best wet heat-treatment temperature is 65 °C, and the crimp number, crimp ratio, and crimp elasticity ratio of PLA/LM-PLA SSCF is 21 per 25 mm, 31.9% and 81.6%, respectively. Moreover, the wet heat-treated PLA/LM-PLA SSCF obtained better fluffy properties. The dry/wet heat treatment maintains the mechanical properties of PLA/LM-PLA SSCF. The performance of the three-dimensional crimped PLA/LM-PLA SSCF is comparable to that of industrialized three-dimensional crimped PET/PTT SSCF, which will expand its application field.

Conflicts of interest

There are no conflicts to declare.

Acknowledgements

Notes and references

1 Z. G. Wang, F. C. Yang, X. S. Zhu and J. Q. Cheng, *Synthetic Technology & Application*, 2007, **22**, 42–44.

2 R. Kotek, *Polym. Rev.*, 2008, **48**, 221–229.

3 Y. X. Zhang, F. Mei, X. Jiang, L. Y. Xie, Q. Lin and H. S. Tian, CN Patent, 104141178, 2014.

4 J. K. Wang, G. M. Jiang, X. H. Liao, Z. Gao and Z. Z. Yang, CN Patent, 111041568, 2020.

5 J. Luo, F. M. Wang and B. G. Xu, *Text. Res. J.*, 2011, **81**, 538–544.

6 T. H. Oh, *J. Appl. Polym. Sci.*, 2006, **102**, 1322–1327.

7 R. S. Stein and F. H. Norris, *J. Polym. Sci.*, 1956, **21**, 381.

8 H. Xiao, M. W. Shi and J. Liu, *J. Text. Res.*, 2008, **8**, 6–10.

9 D. S. Zhang and J. Y. Zhou, *China Text. Leader*, 2016, **12**, 46–51.

10 X. Q. Zhang, Z. J. Xiong, G. M. Liu, Y. A. Liu, R. Wang and D. J. Wang, *Acta Polym. Sin.*, 2014, **8**, 1048–1055.

11 N. C. Nepomuceno, M. N. Barbosa, R. F. Bonan, J. E. Oliveira, F. C. Sampaio and E. S. Medeiros, *J. Appl. Polym. Sci.*, 2017, **135**, 45782–45791.

12 B. Yang, R. Wang, H. L. Ma, X. l. Li, H. Brünig, Z. F. Dong, Y. Qi and X. Q. Zhang, *Polymers*, 2018, **12**, 1353–1364.

13 X. L. Li, X. Q. Zhang, G. M. Liu, Z. K. Yang, B. Yang, Y. Qi, R. Wang and D. Y. Wang, *RSC Adv.*, 2018, **50**, 28453–28460.

14 M. F. Zhang, X. N. Zhao, G. H. Zhang, G. Wei and Z. Q. Su, *J. Mater. Chem. B*, 2017, **5**, 1699–1711.

15 M. M. L. Arras, R. Jana, M. Muhlstadt, S. Maenz, J. Andrews, Z. Q. Su, C. Grasl and K. D. Jandt, *Macromolecules*, 2016, **49**, 3550–3558.

16 P. P. Zhang, X. N. Zhao, X. Zhang, Y. Lai, X. T. Wang, J. F. Li, G. Wei and Z. Q. Su, *ACS Appl. Mater. Interfaces*, 2014, **6**, 7563–7571.

17 T. J. Liu, Y. Q. Guo, Z. F. Zhang, Z. C. Miao, X. Y. Zhang and Z. Q. Su, *Sens. Actuators, B*, 2019, **286**, 370–376.

18 E. W. Fischer, H. J. Sterzel and G. Wegner, *Colloid Polym. Sci.*, 1973, **251**, 980–989.

19 P. H. Hermans and P. Platzek, *Colloid Polym. Sci.*, 1939, **88**, 68–72.

20 H. M. Chen, Y. Shen, J. H. Yang, T. Huang, N. Zhang, Y. Wang and Z. W. Zhou, *Polymer*, 2013, **54**, 6644–6653.

21 B. Na, S. F. Zou, R. H. Lv, M. B. Luo, H. Y. Pan and Q. J. Yin, *J. Phys. Chem. B*, 2011, **115**, 10844–10848.

22 P. Y. Wu, *Shanghai Text. Sci. Technol.*, 2008, **36**, 47–50.

23 W. J. Lin, J. Luo and F. M. Wang, *Synth. Fiber China*, 2010, **39**, 27–31.

24 L. Cai, F. X. Li and J. F. Qian, *China Synth. Fiber Ind.*, 2010, **33**, 18–20.

25 C. M. Wang, R. Wang, Y. S. Chen and D. S. Zhang, *China Synth. Fiber Ind.*, 2009, **32**, 40–42.

26 T. H. Oh, *J. Appl. Polym. Sci.*, 2006, **101**, 1362–1367.

27 S. P. Rwei, Y. T. Lin and Y. Y. Su, *Polym. Eng. Sci.*, 2005, **45**, 838–845.

28 J. H. Kim, S. S. Yang and S. M. Hudson, *Fibers Polym.*, 2011, **12**, 771–777.

29 J. B. Pagrk, K. L. Devries and W. O. Statton, *J. Macromol. Sci., Part B: Phys.*, 1978, **15**, 205–227.

30 J. H. Dumbleton and B. B. Bowles, *J. Polym. Sci., Part A: Polym. Chem.*, 2010, **4**, 951–958.